MULTISPECIES SUBLIMATION OF A COMET INCLUDING THE INFLUENCE OF THE GAS-PHASE ON THERMAL CONDUCTIVITY

C. J. Alexander
Jet Propulsion Laboratory, 4800 Oak Grove Dr., Pasadena, CA 91109
T. I. Gombosi
University of Michigan, 2455 Hayward St., Ann Arbor, MI 48109

Abstract

The heat transfer process that results from gaseous diffusion through the nucleus is shown to play a significant role in modeling comet nuclei. In this paper, a comprehensive comet nucleus model is presented which simulates the efflux of gas from surface and interior layers, The model includes 3 volatile components; CO, CO_2, and H_2O, and a siliceous dust component. Mass, momentum, and energy balance equations are solved at the surface and interior layers. Equations of state for ices based on the latest thermodynamic data; the Brown and Ziegler [1979] relationship for the sublimation of CO_2 and CO at low pressure and the Lowe [1977] expression for water vapor at low pressure are used with the model. Variability in the matrix parameters of density, porosity, friability, tortuosity, pore radius of the matrix, and phase of the interstitial ices, are options explored with the model. Results in the form of total gas production rates are compared with measured cometary light curves from comet P/Halley.

Introduction

Comets are among the most interesting of solar system objects because of their possibly pristine character, yet potential for complex surface geology, complex thermal history, and surface processing to form complex organic refractory material. During it's traversal of deep space, and through a perihelion passage, cometary ices can undergo a variety of changes including changes of phase, sublimation of the material, diffusion of molecules within the nucleus, and changes in the thermal conductivity. These phenomena are strongly influenced by changes in the microtexture of ices of the nucleus during the heating associated with a perihelion passage. Modeling is performed of these processes to determine among other things, the internal temperature evolution and total gas production of the nucleus. These are found by accounting for the feedback effect of heat transport to the nucleus interior, gas transport through and out of the nucleus, and the relative size of a dusty overlayer, or mantle. Significant heating of the icy matrix of the nucleus results in rapid sublimation and buildup of an evacuated silicate layer, however, build up of too thick a mantle inhibits gas production and insulates the interior from the effects of insolation.

The model contains 3 volatile constituents, CO, CO_2, and H_2O, as well as a dust component. The model also explores the effects of a number of different free parameters on cometary outgassing, such as the tortuosity of the porous structure, the porosity itself, the pore radius size, the albedo, and the friability of the matrix. Models of this kind are severely hampered by the lack of constraints. Unknowns include some fundamental properties such as the microtexture of the material, the thermal

conductivity of the material, and the equation of state which governs the sublimation, This model incorporates some versatility in the parameter regimes used. In addition to the ability to tweak some simple parameters such as the albedo and friability, the model also explores some fundamental differences among thermal conductivity models, models of gas kinetic regime, and changes to the equation of state governing gas production. OH measurements from various comets, including comet P/Halley are used to provide constraints on the output of the model, namely the total gas production.

We modeled the thermal conductivity in a way suggested by Smoluchowski [1982] to account for heat transport by the vapor phase within the nucleus. Accounting for heat conduction due to the vapor phase proved to be the most significant change to all the physical parameters which were used with the model, The efficacy of the vapor phase derives from the porosity of the nucleus structure itself. In a very porous structure, latent heat is released when the vapor diffuses to a colder place within the matrix and recondenses. Smoluchowski [1982] predicted the importance of the role of the vapor contained in pores on the conductivity of the nucleus. According to Smoluchowski [1 982] neglect of this important physics would result in a calculated gas production rate which would be anomalously low. Anomalously low values for total comet gas production were what we found until we accounted for the physics of this process.

Nucleus Geometric Construction

The thermal properties of the nucleus are intricately linked to the geometric properties of the matrix, therefore a consideration of the geometric construction of the nucleus on a microscopic level is in order. Comets are possibly formed in a unique manner in which the ices and solids condensed into a disordered structure where the porosity is very large. Greenberg and D'Hendecourt, [1985] have shown that at some point in time ices of carbon monoxide, carbon dioxide, methane, ammonia, water, and assorted other volatiles condensed onto 0.5 pm- 100pm siliceous and carbonaceous grains that had previously condensed out of the solar nebula, There are a, number of different structures suggested for these grains, but typically, a small, stony, porous core of siliceous, carbonaceous or perhaps metallic origin is overlain with ices. A number of these cores, melded together, form an idealized cometary dust grain [Fechtig and Mukai, 1985].

The nominal, water ice matrix is composed of an oxygen atom of one of the molecules acting as the center of a regular tetrahedron, the angles of which are occupied by other oxygen atoms. Every oxygen atom on the summit of a tetrahedron is the center of another tetrahedron oriented upside down with respect to the first. Distortion of the bond angle between the water molecules causes a new ice structure to be formed. The structure is hexagonal if the angles of the tetrahedral are superposed. The structure is cubic if the second tetrahedron is rotated by an angle of 600 . The

structure is amorphous if no long-range correlation exists between the orientations of the tetrahedra. Pristine ice at lowest temperatures (T<136 K) is amorphous. Cubic ice forms at temperatures between 110 and 150 K. At 200 K cubic ice irreversibly transforms to hexagonal ice. Experiments show amorphous ice at low temperatures is stable, and can accommodate the hosting of guest volatiles of another species,

The structure of a comet nucleus may be porous at many different size scales, from the angstrom to the millimeter size range. Condensing water vapor does not always adopt the nominal tetrahedral structure, thus there will be pores as a feature of the water matrix. On a larger scale, the material does not compact as it accumulates resulting in a matrix with a macrotexture likened to a woolen carpet. Silicate grains accumulating under vacuum conditions are found to have a "birds nest" structure, a loosely packed aggregate structure where the grains are vesicular in form, This texture produces voids in the structure which can be likened to channels, on the order of microns to millimeters in scale. Ice which condenses at low temperatures (<100 K) may have an amorphous, or glass-like form, and still have a large porosity, on the scale of angstroms to microns.

The model explains the simultaneous outgassing of different volatile species by assuming the comet to be structured as a porous medium containing water ice, and sufficient unencapsulated CO and C02 to produce significant sublimation. A schematic of the structure assumed is shown in figure 1. Upon heating, gaseous volatiles filter through the porous overlying dust and ice layers and escape. The model does not yet account for the transition from amorphous to cubic or hexagonal ice, nor have we constructed the model with the capacity to change porosity in mid-calculation, Failure to account for these time-dependent processes in the model may prove to be significant,

The Thermal Model

Macroscopic Heat balance

To mode] this structure, an approach was used which is based upon that of Brin and Mendis [1979], and Houpis et al. [1985], with the assumption of a chemically differentiated nucleus, That is, it is assumed that an initially homogeneous layer composed of a mixture of molecular ices becomes differentiated upon heating into sub-layers (mantles) which are evacuated of the more volatile ices from the layer below. In a mixture of CO, C02, dust and water, for example, where CO is the most volatile of the constituents, and C02 the second most volatile, the nucleus will eventually separate into layers, the first of which is constituted of dust, a second which is constituted of water and dust, a third which is constituted of C02, water, and dust, and finally an undifferentiated core constituted of CO, C02, H20 and dust. Figure 1 depicts this structure. For ease of calculation, the mode] assumes that

there is a surface of sublimation for each volatile constituent, and that surface exists only at the uppermost edge of the layer, there is no sublimation within a layer. For example, water sublimation occurs only along the crossectional area of the interface between the layer constituted of dust and the layer constituted of dust and water,

With this construct, energy balance equations can he applied to four nucleus interfaces, the nucleus surface, the water layer interface, the C02 layer interface, and the CO layer interface. It is assumed that heat is not conducted to the deep interior of the comet and that the heat conducted to the interior is equivalent to the total energy available for sublimation. The energy balance equation at the nucleus surface is written as the balance between the absorbed solar radiation flux and a combination of blackbody reradiation, vaporization of surface volatiles, and conduction of heat to the interior:

$$\frac{(1-A)}{d^2} J = \varepsilon \sigma T_4^4 + \frac{\partial}{\partial z}\left(\kappa(T)\frac{\partial T}{\partial z}\right)_{z=0} \qquad 1$$

where ε is the emissivity, σ is the Stefan-Boltzmann constant, N_A is Avogadro's Number, T is the temperature, and T4 is the surface temperature. The first term of the left hand side is the absorbed radiation flux, where (J) is the solar insolation, (A) is the albedo of the material, and (d) is the distance from the sun. The first term of the right hand side is the net blackbody re-radiation of the body, the second term is the divergence of the heat flux vector in one dimension.

The sublimation rate of a given species, dq, is equivalent to Ldm, where L is the latent heat per mole and m is the mass undergoing transition. Dm is also equivalent to the gas production rate,. $\dot{Z}$. Since the gas is considered to be sublimating from an area comprising the surface of a given layer, the gas flux is multiplied by the fraction of area, f, of the volume undergoing sublimation, The heat flux at the surface therefore is;

$$dq_{surface} = \sum_{\text{s=all volatiles}} \frac{L_s f_s \dot{Z}_s}{N_A} \qquad 2$$

This yields a surface energy balance equation of

$$\frac{(1-A)}{d^2} J = \varepsilon \sigma T_4^4 + \sum_{\text{s=all volatiles}} \left(\frac{L_s f_s \dot{Z}_s}{N_A}\right) \qquad 3$$

Temperatures of the interior layers are obtained via integration of the energy balance expressions for the other three interfaces. The constant of integration is equivalent to the energy of sublimation

Interior layer temperatures are dependent upon the values chosen for the conductivity of the layer, $\kappa(T)$. In this paper we present the results of models which make use of two different regimes of thermal conductivity. Currently we run the model with either of these two regimes. This method provides the groundwork for allowing the program to change regimes in mid-calculation. In the future this will allow us to model time-dependent effects such as the change from amorphous to crystalline ice. In the first regime the thermal conductivity was modeled after [Klinger, 1981], where $\kappa(T) = \alpha^*/T$. A value of a* =5.67x10^4 ergs/cm/sec was used, to reflect the fact that the nucleus matrix material *is* more irregular and inhomogeneous than that laid down in the laboratory under controlled conditions, The thermal conductivity of the C02 layer is taken to be identical to that of the water layer (et* *= et*). Thus expressions for the temperatures of the two interior layers are given by:

$$T_2 = T_1 \exp\left(\frac{\Delta_1}{\alpha^{**}}\left[\frac{L_{co} f_{co} \dot{Z}_{co}}{N_A}\right]\right) \qquad 4$$

$$T_3 = T_2 \exp\left(\frac{\Delta_2}{\alpha^{*}}\left[\sum_{s=co,co_2} \frac{L_s f_s \dot{Z}_s}{N_A}\right]\right) \qquad 5$$

For the dust layer, $\kappa(T)$ *is* taken to be constant, κ_O, where κ_O is 60 ergs/cm/K/sec measured from silicate moon rocks [Fountain and West, 1970]. Therefore the surface temperature is given by

$$T_4 = T_3 + \frac{\Delta_3}{\kappa_o}\left[\sum_{s=\text{all volatiles}} \frac{L_s f_s \dot{Z}_s}{N_A}\right] \qquad 6$$

This regime is characterized by the fact that the thermal conductivity of the ice component is an inverse function of temperature.

In the second regime of thermal conductivity, the conductivity of the icy component is modeled as an effective thermal conductivity which accounts for the effects of the vapor phase upon the heat conduction within the layer, after Smoluchowski [1982]. Gaseous diffusion through the nucleus results in a heat transfer process similar to that of conduction where the gas exchanges heat with the solid material and reduces the thermal gradient in the interior. Smoluchowski [1982] predicted the effective thermal conductivity of porous ices of various compositions as functions of temperature and porosity, and showed that the dependence of this effective conductivity on temperature is more nearly a direct relationship rather than an inverse relationship. At present we model this effective thermal conductivity as a linear relationship with two slopes; for temperatures less than 189K, $m_{1,icy}$=280 ergs/sec/cm/K^2, $b_{1,icy}$ =1.1x 10^{4}ergs/see/cm/K, otherwise $m_{2,icy}$=800 ergs/sec/cm/K^2, $b_{2,icy}$ = 1.1x104 ergs/sec/cm/K, . More correctly the effective thermal conductivity is

the geometric addition of the thermal conductivities of each volatile, both for the medium of the ice/grain mixture and the vapor phase, and is not a linear relationship.

Recent work by Cahill et al., [1992] provides the thermal conductivity of amorphous silicate solids at very low temperatures (30 K). This thermal conductivity may also be modeled as a linear relationship with two slopes; for temperatures less than 175K, $m_{1,silicate}$= 508 ergs/sec/cm/K^2, $b_{1,silicate}$ = 5.833x 10^3 ergs/sec/cm/K, otherwise $m_{2,silicate}$ = 200 ergs/sec/cm/K^2, $b_{2,silicate}$ = 6.0x 104 ergs/sec/cndK. Only one run was performed with this change to the silicate thermal conductivity (see figure 6), however work with this relationship suggests that the thermal conductivity of the silicate component may be more consistent with that of disordered crystals. In this regime, where the thermal conductivity is a linear relationship with temperature, the temperatures of the interior layers are given as a quadratic,

$$\frac{m}{2}T_{2,3,4}^2 + bT_{2,3,4} - G = O$$

where m and b are the slopes and intercepts given above appropriate for the layer, and

$$G = \frac{m}{2}T_{1,2,3}^2 + \left[bT_{1,2,3} + \sum_{s=[(2,3,4)-1]\ \text{volatiles}}^{1} \frac{f_s \dot{Z}_s}{N_A} \right] \qquad 8$$

Values for other parameters are given as follows, and in table 1. As the nominal case, density values appropriate for hexagonal ice were adopted. The density of pure CO at extremely low pressures is not available in standard references and was derived. CO packs in a face-centered cubic structure near temperatures of 23 K [Barrett and Meyers, 1965] therefore the density of 2.106 g/cm^3 can be obtained, where Sanford and Allamandola, [1988], give, the size of the CO lattice site in pure CO as 3.4 x 3.4 x 4.6 $Å^3$. The latent heat release for the water phase transition is assumed constant with temperature (Newitt et al., [1956]), L_{H2O} = 5.OX101 1 ergs/mole. Laboratory measurements of latent heat for pure C02 show a linear relationship with temperature, where the slope m_{LCO2} = -3.0308x 108 erg/mole/K and the intercept b_{LCO2} = 3.0915x 10^{11} erg/mole, [Newitt et al., 1956]. The range of laboratory measurements used by Newitt et al., [1956] (143 -217 K) are higher than the corresponding ranges for CO used by the model, nevertheless it is assumed that the relationship still holds. The latent heat of CO is also linear, with m_{LCO} = -3.6949x108 erg/mole/K and b_{LCO} = *1.0496x* 1011 erg/mole, Leah [1956]. The temperature range of laboratory measurements used by Leah [1956] for this determination of L_{CO} was 5S-62 K and this is consistent with the temperatures in the core.

Equations Of State For Low Pressure Ices

Different regimes were also used to account for the relationship of the temperature dependence of vapor pressure for the various volatile constituents. The Clausius-Clapeyron relation, formulated for an ideal gas over a plane surface, may not be an appropriate standard in the astrophysical environment. To find the vapor pressure, the Clausius-Clapeyron relationship must be integrated. The constant of integration is evaluated via laboratory measurements, which are performed for vapor pressure changes over a wide temperature range. Use of the latest thermodynamic information may provide more accurate estimates of the sublimation rates. Goff and Gratch [1946] integrated the Clausius-Clapeyron equation for the departure of water vapor from an ideal gas and performed a curve fit to numerically tabulated salutation vapor pressures, to give another relation for water vapor, namely the Goff-Gratch relationship (valid for temperatures in excess of 2.00 K). Recently, for ease, speed, and efficiency in computation, polynomial approximations to the Goff-Gratch equation have been performed. One of these, Lowe [1 977], recommended by Gibbons, [1990], for speed of calculation where multiple calculations of the saturation vapor pressure are required and given below, is used with the model.

$$P_{h2o}(hPa) = \left(a_0 + T\left(a_1 + T\left(a_2 + T\left(a_3 + T\left(a_4 + T\left(a_5 + a_6 T\right)\right)\right)\right)\right)\right) \qquad 9$$

Similarly, Brown and Ziegler, [1979], presented curve fits to tabular data of the heat of vaporization, and the heat capacity for CO and C02 in low temperature low pressure regimes,

$$P_{co2}(\text{torr}) = \exp\left[A_{0_{co2}} + \frac{A_{1_{co2}}}{T} + \frac{A_{2_{co2}}}{T^2} + \frac{A_{3_{co2}}}{T^3} + \frac{A_{4_{co2}}}{T^4} + \frac{A_{5_{co2}}}{T^5} \right] \qquad 10$$

$$P_{co}(\text{torr}) = \exp\left[B_{0_{co}} + \frac{B_{1_{co}}}{T} + \frac{B_{2_{co}}}{T^2} + \frac{B_{3_{co}}}{T^3} + \frac{B_{4_{co}}}{T^4} + \frac{B_{5_{co}}}{T^5} \right] \qquad 11$$

The coefficients for these expressions are given in table 2.

Gas Production

Given the geometric construction of the model, as an ice/grain matrix with a large porosity, and the rarefied nature of the gas, the mean free path of molecular flow will be longer than the dimensions of the flow space. An expression for gas flux for molecular flow in the Knudsen regime, therefore, is required. The gas flux of species s is given by

$$F_s = \frac{4}{3}\sqrt{\frac{2kT_s}{\pi m_s}} r_0 \frac{dn_s}{dz} \qquad 12$$

where the geometric factor of 4/3 represents the permeability of the presumed medium, $r0$ is the mean pore radius, m_s and T_s are the mass and temperature of species s, respectively. In steady flow, F must be constant, therefore the density gradient is uniform and can be replaced by $\Delta n/l$ where l is the length of an assumed tube and Δn *is* the difference in density between the ends of the tube. In this expression 1 is just the tortuosity times the layer thickness A. As the nominal case, the number density, n_s, for each species s is taken from the Clausius/Clapeyron expression for the mass undergoing transition:

$$\frac{d \ln P}{dT} \frac{L(T)}{RT^2} \qquad 13$$

where P *is* the vapor pressure, L is the latent heat, and R is the universal gas constant. The latent heat is assumed to be a linear function of temperature, where values for the constants m_s and b_s were given earlier. Upon integration and substitution;

$$n_s = n_0 \left(\frac{T_0}{T_s}\right)^{\left(1-\frac{m_s}{N_A k}\right)} \exp\left[\frac{b_s}{N_A k}\left(\frac{1}{T_0} - \frac{1}{T_s}\right)\right] \qquad 14$$

where T_0 is a species' reference temperature. Consequently

$$\dot{Z}_s = m_s \frac{4}{3}\sqrt{\frac{2kT_s}{\pi m_s}} r_0 \frac{n_s}{t_m \Delta_s} \qquad 15$$

where *ms is* the mass of the species, the length of the tube is given by the mantle thickness A times the tortuosity factor, t_m. The number density can also be taken from the Lowe [1977] expression (equation 9) for water vapor, and from the Brown and Ziegler [2979] expressions (1 O, 11) for CO_2 and CO.

Benkhoff and Huebner [1995] demonstrated the importance of heat transport to the body by multi-directional gas phase diffusion through the interior of the nucleus for a multicomponent gas. A gas production rate can be derived which specifically applies to a multicomponent gas in the Knudsen regime and correctly accounts for a second component of diffusion which overcomes resistance to diffusion or loss of momentum by the gaseous flow to the walls. This second component of diffusion (designated non-equimolar flux or diffusion slip flux, Kaviany, [1 9911, Mason and Malinauskas, [1983], and Cunningham and Williams, [1980]) accounts in a more sophisticated manner for the permeability of the material through which the gas must flow and is

dependent upon the species' concentration gradient as well as the temperature gradient within the medium. The complete expression for Knudsen diffusion for a multicomponent gas in a porous media can be derived from the 13-moment Boltzmann equation and includes a multispecies diffusion coefficient which is highly dependent upon the assumed structure of the medium. A version of the model presented here was developed, which accounted for the physics of multispecies diffusion. Results were returned by the more sophisticated version of the model, not presented here, were qualitatively similar to results which are presented here. This leads us the conclusion, drawn later in the paper, that in order to effectively reproduce overall cometary gas production, the effects of gas phase diffusion must also be accounted for in the macroscopic thermal conductivity expression.

Growth of the Mantle

From the expression for conservation of mass, the change of mass with time for a given layer can be expressed as the density, ρ, times the volume change: the area, A, times the change in the mantle thickness, $d\Delta/dt$. The change in mass with time can also be expressed by the mass flux, mF, where F is the gas flux, and the gas flux F *is* related to the gas production rate via $mF=fZA$,:

$$\frac{dM}{dt} = A\rho\frac{d\Delta}{dt} = mF \qquad 16$$

The rate of change of the mantle thickness (for layer three in the equation below) is the rate at which sublimation occurs at the bottom of the level, minus the rate at which the top of the level erodes;

$$\frac{d\Delta_3}{dt} = \frac{1}{A\rho_{h_2o}}\frac{dM_{h_2o}}{dt} - \frac{1}{A\rho_d}\frac{dM_d}{dt} \qquad 17$$

where ρ_S' is the fraction of mass undergoing sublimation inside a volume element, $\rho_S'=\rho_S\eta_S$, and η_S is the fractional volume undergoing sublimation, The change of mass of the dust layer (dM/dt) depends upon the amount of gas flowing through it:

$$\frac{dM_d}{dt} = \chi_1\frac{dM_{h2o}}{dt} + \frac{\chi_1}{\chi_2}\frac{dM_{co_2}}{dt} + \frac{\chi_1}{\chi_3}\frac{dM_{co}}{dt} \qquad 18$$

where χ_i is the mass ratio of constituent (i) to water, The porosity is derived via the volume of ice versus the total volume available. Adjustment of the dust mass ratio fixes the relative hardness of the silicate mantle with respect to the gas. Perfect drag is assumed between the gas and dust grains after Finson and Probstein [1968]. Upon substitution for $\rho s'$ and rearrangement, a set of three actuations for three unknowns $\Delta 1, \Delta 2, \Delta 3$ *is* obtained:

$$\frac{d\Delta_3}{dt} = \frac{\dot{Z}_{h2o}}{\rho_{h2o}\eta_{h2o}} - \frac{\chi_1\dot{Z}_{h2o}}{\rho_d} - \frac{\chi_2\dot{Z}_{co_2}}{\rho_d} - \frac{\chi_3\dot{Z}_{co}}{\rho_d} \qquad 19$$

$$\frac{d\Delta_2}{dt} = -\frac{\dot{Z}_{co_2}}{\rho_{co2}\eta_{co2}} - \frac{\dot{Z}_{h2o}}{\rho_{h2o}\eta_{h2o}} \quad 20$$

$$\frac{d\Delta_1}{dt} = -\frac{\dot{Z}_{co}}{\rho_{co}\eta_{co}} - \frac{\dot{Z}_{co_2}}{\rho_{co2}\eta_{co2}} \quad 21$$

where the area fraction of sublimation is incorporated into the term $\dot{z}_i$. This set, along with expressions for gas production rate yield the core equations for the model; 3,4,5,6,19,20,21. The equations are solved numerically for the mantle thicknesses *(A)*, and layer temperatures. Values for these parameters become initial conditions for the next step along the trajectory in a simulated cometary orbit,

Results

Figures 2-6 show examples of the brightness histories returned by the model. Because of the extensive CPU time required to complete an orbit, it should be noted that while some of the calculations were carried to 6 orbits, in many cases the calculation was interrupted before completing as much time. In each figure, the top left panel shows the evolution of the thicknesses of the mantles, dust (denoted "delta 3"), water ("delta 2"), water/CO_2 ("delta 1 "). Temperature evolution is shown in the top right panel, while the gas production solution is shown in the bottom left. Individual species' gas production solutions sum to give the total gas production rate, plotted in the bottom right panel. The total gas production ($molecules \cdot sec^{-1}$) is found by multiplying the total gas production rate by an active area, taken to be 50 km^2, after Halley's comet, and dividing by the mass of gas. For comparison, OH measurements of comet P/Halley as determined by the International Ultraviolet Explorer are also shown [from Roettger et al., 1990].

In general, the solutions evolve as follows, the innermost mantle grows on the initial orbit from nothing to several meters very quickly as the most volatile element sublimes. Over subsequent perihelion passes, this mantle grows at a substantially slower rate. This means that efficient and rapid sublimation of the lowest level is choked off early and sublimation shifts to upper layers. The middle mantle thickness, marked by open squares in the figures, initially grows to tens of centimeters and grows steadily but ever more slowly over subsequent orbits. The top mantle, marked by open circles in the figures, initially grows to a thickness of a few centimeters then shrinks slightly on the outbound pass toward aphelion when the rate of erosion of the top layer overtakes the rate of sublimation. The feedback effect of dust mantle thickness, gas production and interlayer temperature is as follows, the insulating effect of a thick mantle eventually chokes off the gas production of the lower layer, and

results in a higher temperature in the layer. Rapid gas production, analogous to effective drying of the layer, results in cooler temperatures in the layer but more rapid erosion of the layer. An increase in the overall heat flux as the comet approaches perihelion drives the temperatures up and hence the gas sublimation rate. These feedback effects affect the model differently depending upon the construction of the matrix, it's density, porosity, and hardness.

Figures 2 & 3 show results returned by the model in which the regime of thermal conductivity with an inverse temperature dependence. Figure 2 shows a "water" comet of composition 80% water, 10% CO, 5% CO_2 and 5% dust. The general result returned by this model is moderately high volatile activity at outlying distances within the solar system, but low activity at perihelion compared with the water vapor activity of Halley's comet as shown in bottom right panel of the figure. The water solution, marked by open circles, remains insignificant until within the inner solar system. C02, marked by open squares, is effervescent over a larger, extended region of the orbit. CO is effervescent over the extent of the trajectory. As the dust mantle grows there is clearly a dip in the gradient of volatile production related to insulating effects. The comet becomes bald again near the aphelion regions following the first perihelion pass, but retains a thicker and more extensive dusty mantle on subsequent passes.

Figure 3 shows a case where the Brown/Ziegler equation of state was used for the vapor pressure of C02, while the Clausius/Clapeyron equation was used for the vapor pressure of the other volatiles. Conditions of high tortuosity, high porosity and low friability were chosen to maximize the total production at perihelion. This case comes to higher equilibrium temperature values for the interior because the saturation carbon dioxide vapor pressure occurs at a higher temperature. Temperatures were too low during the cruise passage of the comet, from aphelion to the inner solar system, for a substantial carbon dioxide production rate. The 'water production rate exhibits a steep gradient from the cruise portion of the orbit to perihelion. Production values such that the mantles are thin and the comet is bald for several perihelion passages. The case in which the Brown/Ziegler equation of state was used for the vapor pressure of CO while the Clausius/Clapeyron equation was used for the other volatiles is qualitatively similar and is not shown. The case in which the Lowe equation of state is used for water (not shown), with the Clausius/Clapeyron equations for CO and C02, produces very effervescent water production rates.

Figure 4 shows the results of the model presented here for a water-CO2-dust comet where the effective conductivity has a direct relationship with temperature. The result shows the efficacy of accounting for the thermal conductivity of the gas phase with this model. Gas production returned by the model at perihelion is increased 10-fold, bringing the total production much more nearly in line with the data. Subsequent perihelion passes, however, reveal that the total production falls off rapidly from the initial pass, and the dusty overlayer increases from 500 μm to 1000 μm. This comet is bald for much of it's orbit, including it's passage within the inner solar system. In this comet, there

is a high degree of water available for sublimation, and relatively little resistance to the flow because the hardness of the silicate dust is low. The layers effervesce readily, sublimation exceeds erosion of (he surface, and hence the dust mantle is thick at perihelion. In cases where there is less water available for sublimation, there is not as much efflux at perihelion, and the dust mantle is thinner, but still in existence.

Figure 5 shows use of an effective thermal conductivity for the dust component of a water-dust comet where the dust is considered to be of an amorphous structure [Cahill et al., 1980]. Gas production returned by the model at perihelion is increased 30-fold, again bringing the total production much more nearly in line with data.

Hundreds of runs of this model have been performed, and analysis of these runs have lead to some generalities which can be discussed, Moderate amounts of secondary volatiles, such that the water abundance remained high, was all that was needed for a high level of productivity at perihelion. Comets of great abundances of either CO or C02 neither returned larger production rates nor thin mantles. The porosity of the matrix had a significant and ubiquitous effect. With large porosity, the comet output diminished. For highly porous comets, gas production and erosion, proceeded rapidly, there was no significant buildup of mantles, and the comet was cool. At perihelion, therefore, the comet was so cool as to produce little water vapor, and that condition lead to low total efflux at perihelion. In general, baldness was exhibited in all the comets, but there were no cases wherein baldness was exhibited at perihelion. There was no blow off of mantles near perihelion. Dust mantles were built up but, characteristically, they were not blown off around perihelion; rather the opposite occurred, namely that the dust mantles diminished at the aphelion portions of the orbit. This is explained by the fact that the rate of erosion at aphelion is greater than the rate of sublimation at aphelion, but it suggests that erosion of the surface at aphelion is a feature of comet outgassing.

Discussion

In spite of the low overall gas production returned by the model, the results can be discussed in light of what other models show. Previous models, such as Fanale and Salvail [1984], have found that a microscopically thick dust mantle cannot be produced in a realistic amount of time by a model which accounts for features such as rotation of the nucleus and diurnal heating effects. Such a model requires hundreds of perihelion passes to produce a fully developed mantle in a long period (Halley-type) comet. This kind of model was unable to produce an Enke-type short period comet, because Enke's comet is mantled. Other models (including the one presented here) such as Horanyi et al. [1984] do produce thick mantles for what is essentially an outgassing slab constantly facing the sun. Unfortunately, in these models, regions of space wherein the mantle is built most efficiently seem to occur in the wrong location. In other words, thick mantles accumulate at perihelion, where gas

production is strongest, and thin mantles or baldness occurs where sublimation is weakest. Data analysis shows, however, that it is the area just under the jets where ices are presented directly to space, that is, at perihelion the surface cracks open and the freshly exposed material sublimates directly to space. The danger, in modeling, of building too thick a mantle which cannot be removed and which effectively chokes off gas production was pointed out by Prialnik and Bar-Nun [1 988]. Their model required explosions of the underlying ice during phase transitions to remove enough overlying material to produce efficient gas production. Taken together these results suggest that the mantle building process is perhaps being modeled incorrectly. We suggest the importance of the presence of organic refractories.

There are a few experiments being done with organic refractories, and these studies have made a few measurements of their properties. In the recent KOSI-9 space simulation experiment, Grun et al., [1993], ices of varying compositions, containing small amounts of organic carbons, silicates and/or metals, were irradiated with photons and a rudimentary crust of refractories was formed, It has been shown [Jenniskens et al., 1993] that irradiated ice samples of various mixed molecular icy compositions with UV photons and low energy ions can form sophisticated hydrocarbons such as glycerol. Jenniskens et al. [1993] showed that the porosity of the refractory residue was such that sublimation occurred within cracks in the residue and not elsewhere. Figure 6 gives an indication of the expected result of the addition of a carbonaceous layer to the model. Figure 6 shows two cases from the model, with three volatiles, CO, C02, and H20. In one case, the global friability (breakability) of the dusty overlayer is high, and the other case the global friability is decreased substantially. In the first case, because the overlayer is easily breakable, a dusty, siliceous mantle develops only near the perihelion pass, where sublimation is more rapid than the erosion of the surface. Otherwise the comet is bald, with ice exposed directly to space. In that case, sublimation to space is not inhibited, interior temperatures are cool by the time of perihelion, and there is little dramatic increase in sublimation, When the overlayer is less easily breakable, the dusty layer thickens faster along the orbit and remains thick, the radiating temperature is higher, and the sublimation becomes more dramatic only during the perihelion pass where sublimation is more rapid than erosion of the surface. A thin refractory layer of low porosity would inhibit sublimation during middle solar system portions of the orbit, allowing interior temperatures to increase. At perihelion, gas pressure from sublimation will widen the cracks in the layer, allowing increased activity at that time. A layer of this kind will incorporate the insulating properties of a dusty mantle without incorporating the propensity to grow so thick as to cut off activity.

The significance of changes to the thermal conductivity, and it's affect on the model, suggest that time dependent effects and geology may play an important role in cometary physics. Comet ice may initially be a poor conductor because of its porous character, however, the slightest melting may induce a dramatic increase in the thermal conductivity because the elements of the matrix have closer

contact with each other. This implies that thermal conductivity may be a function of evolution of the matrix and the temperature of the interior. Thermal conductivity is also a function of porosity, since pores open when the material heats and close via condensation when the material cools. Porosity, as a parameter, is affected by the phase of ice and how the ice evolves with time and temperature. Blake et al., [1991] have shown that an initially amorphous mixed molecular ice, which a comet nucleus undoubtedly is, can undergo devitrivication into a clathrate and a pure component of secondary ice at a moderate temperature (130 K). Such a structure takes on a new porosity because occluded molecules have been driven out, making larger passages for subliming gases. These compounds can exist next door to segments of amorphous ice which did not undergo devitrivication, and which retain the original porosity, Additionally, Jenniskens and Blake, [1994], have shown that there may not be a clear separation between amorphous and non-amorphous phases but that the amorphous component may be intimately mixed with cubic ice. These important geochemical processes suggest that accounting for the time dependent geology of nucleus evolution, and its effect on the thermal conductivity and gas kinetic properties of the volume is a significant modeling consideration.

Conclusions

Initial results returned for this model reflected an unrealistically low total gas production rate. Steps taken to correct this problem indicated that consideration of the transport of latent heat by the vapor phase is important to the physics of heat transport within the nucleus, as is consideration of the thermal conductivity and structure of the silicate component. The process of building a cometary mantle was examined with the results of this model. Models of comet nuclei have, in the past presupposed the necessity of the buildup of thick mantles over time, based on cometary albedo measurements including those of comet P/Halley. But presumptions of this sort may be flawed. The model presented here is successful at showing appropriate asymmetries in gas production about perihelion, and permanent, thick mantles which are built readily, early, and are effective at choking off gas production. The desired physics is an insulating component which contributes to raising the temperature of the interior, but which is also thin and permeable such that it can be removed at perihelion. That component may be supplied by an organic refractory constituent which comes about as a result of radiation processing of the comet surface over time.

The need to account for time-dependent physical processes such as surface geology and geochemistry in the outgassing evolution was also shown to be significant. The porosity and microtexture of the nucleus, as well as phase changes of the constituents, play a significant role in the fundamental properties such as the sublimation parameters and thermal conductivity. These properties change significantly with the warming of the nucleus. Taken together the results of this

paper suggest that a comet is not a pristine, unprocessed body but a body with perhaps a significant evolution, an evolution which future models must capture.

References

Benkhoff, J. and W. Huebner, Influence of the Vapor Flux on Temperature, Density, and Abundance Distributions in a Multicomponent, Porous, Icy Body, *Icarus*, in press.

Barrett C. S., and L. M. Meyer, Phase Diagram of Argon-Carbon Monoxide, *J. Chem. Phys.*, **43**, 3502-3506, **1965.**

Blake D., L. Allamandola, S. Sanford, D. Hudgins, F. Freund, Clathrate Hydrate Formation in Amorphous Cometary Ice Analogs in Vacuo, *Science*, 2S4, 548-551, 1991.

Brin G.D. and D.A. Mendis, Dust Release and Mantle Development in Comets, *Astrophys. J., 229, 402-408, 1979.*

Brown G.N., Jr., and W.T. Ziegler, Vapor Pressure and Heats of Vaporization and Sublimation of Liquids and Solids of Interest in Cryogenics Below 1 -atm Pressure, *Adv. Cryogenic Eng., 25, 662-270, 1979.*

Cahill, D.G., S.K. Watson, and R.O. Pohl, Lower limit to the Thermal Conductivity of Disordered Crystals, *Phys. Rev. B*, 46, 6131-6140, 1992.

Cunningham R.E., and R.J.J. Williams, *Diffusion in Gases and Porous Media*, Plenum Press, New York, 1980.

Fanale, F.P. and J.R. Salvail, An Idealized Short-Period Comet Model: Surface Insolation, H20 Flux, Dust Flux, and Mantle Evolution, *Icarus*, 60, 476-511, 1984.

Fechtig H., and T. Mukai, Dust of Variable Porosities (Densities) in the Solar System, in Ices *in the Solar System*, J. Klinger, D. Benest, A. Dolphus, and R. Smoluchowski (eds.), D. Reidel, Dordrecht, 251-259, 1985.

Finson M. I.. and R.F. Probstein, A Theory of Dust Comets I. Model and Equations, *Astrophys. J.*, **154**, 327-352, 1968.

Fountain J.A. and E.A. West, Thermal Conductivity of Particulate Basalt as a Function of Density in Simulated Lunar and Martian Environments, *J. Geophys. Res.*, 75, 4063, 1970.

Gibbins C. J., A Survey and Comparison of Relationships for the Determination of the Saturation Vapour Pressure over Plane Surfaces of Pure Water and of Pure Ice, *Annales Geophysical, 8, 859-886, 1990.*

Greenberg J.M. and L.B. D'Hendecourt, Evolution of Ices from Interstellar Space to the Solar System, *Ices in the Solar System*, J. Klinger, D. Benest, A. Dolphus, and R. Smoluchowski (eds.), D. Reidel, Dordrecht, 1985.

Goff, J. A., and S. Gratch, Low Pressure Properties of Water from -160 to 212 F, *Trans. ASHVE, 52, 95-121, 1946.*

Grun, E., J. Gebhard, A. Bar-Nun, J Benkhoff, H. Duren, G. Eich, R. Hische, W. Huebner, H.U. Keller, G. Klees, H. Kochan, G. Kolzer, H. Kroker, E. Kuhrt, P. Lammerzahl, E. Lorenz, W.J. Markeiwicz, D. Mohlmann, A. Oehler, J. Scholz, K.J. Seidensticker, K. Roessler, G. Schwehm, G. Steiner, K. Theil, and H. Thomas,

Development of a Dust Mantle on the Surface of an Insolated Ice-Dust Mixture: Results from the KOSI-9 Experiment, *J. Geophys. Res.,* 98, 15,091-15,105, 1993.

Horanyi M, T.I. Gombosi, T.E. Cravens, A. Korosmezey, K. Kecskemety, A.F. Nagy, and K. Szego, The Friable Sponge Model of a Cometary Nucleus, *Astrophys. J., 278, 449-455, 1984.*

Houpis, H.L., W.-H. Ip, and D.A. Mendis, The Chemical Differentiation of the Cometary Nucleus: 'I'he Process and its Consequences, *Astrophys.J , 295, 654-667,* 1985.

Jenniskens, P., G.A. Baratta, A. Kouchi, M.S. de Groot, J.M. Greenberg, G. Strazzulla, Optical Constants of Organic Refractory Residue, *Aston. Astrophys., 274,653-661, 1993.*

Jenniskens, P., and D.F. Blake, Structural Transitions in Amorphous Water Ice and Astrophysical Implications, Science, 265, 753-756, 1994.

Kaviany M., *Principles of Heat Transfer in Porous Media,* Springer-Verlag, New York, 1991.

Klinger J., Some Consequences of a Phase Transition of Water Ice on the Heat Balance of Cometary Nuclei, *Icarus,* 47, 320-324, 1981.

Leah, A. S., in *Thermodynamic Functions of Gases,* F. Din (cd.), Butterworth's Sci Pub., London, 135, 1956.

Lowe, P. R., An Approximating Polynomial for the computation of Saturation Vapor Pressure, *J. Appl. Meteorol.,* **16,** *100-103, 1977.*

Mason E.A. and A.P. Malinauskas, Gas *Transport in Porous Media: The Dusty-Gas Model,* Elsevier, New York, 1983.

Newitt, D. M., M.U. Pai, and N.R. Kuloor, in *Thermodynamic Functions of Gases, F.* Din (cd.), Butterworth's Sci Pub., London, 102, 1956.

Poirier J. P., Rheology of Ices: a Key to the Tectonics of the Ice Moons of Jupiter and Saturn, *Nature, 299, 683-688, 1982.*

Prialnik D. and A. Bar-Nun, The Formation of a Permanent Dust Mantle and Its Effect on Cometary Activity, *Icarus, 74, 272-283, 1988.*

Rickman, H., The Thermal History and Structure of Cometary Nuclei, *Cornets in the Post-Halley Era, Vol. 11,* R. I.. Newburn, Jr., et al. (eds.), Kluwer, the Netherlands, 733-760, 1991.

Roettger E.E., P.D. Feldman, M. F. A'Hearn, and M.C. Festou, Comparison of Water Production Rates from UV Spectroscopy and Visual Magnitudes from Some Recent Comets, *Icarus, 86, 100-114,* 1990.

Sanford S.A. and L.J. Allamandola, The Condensation and Vaporization Behavior of H_2O:CO Ices and Implications for Interstellar Grains and Cometary Activity, *Icarus, 76,201-224, 1988.*

Smoluchowski R., Heat Transport in Porous Cometary Nuclei, *J. Geophys Res. A. Supp., 87, 422-424, 1982.*

Stevenson R., Compressions and Solid Phases of C02, CS2, COS, 02, and CO, *J. Chem. Phys.,* 27, 673-675, 1957.

water vapor Lowe [1977]	C02 Brown & Ziegler [1979]	c o Brown & Ziegler [1979]
a_0=6. 109177956	$A_{0,co2}$=1 80741181	$B_{0,co}$=21 ,3807649
a_1=5.03469897x10^{-1}	$A_{1,co2}$=-7.69842078 x10^{2}	B] $_{,co}$=-2.570647x10^{3}
a2=l.886013408x 10-2	$A_{2,co2}$=-1.21487759x10^{4}	$B_{2\ co}$=-7.78129489x10^{4}
a3=4. 176223716x 10'4	A3 $_{co2}$=2.7350095x10^{5}	$B_{3\ co}$=4.32506256x10^{6}
a4=5.82472028x10 $^{-6}$	$A_{4,co2}$=-2.9087467x10^{6}	B4 $_{co}$=-1.20671368x 108
a_5=4.838803174x10^{-8}	$A_{5,co2}$=1.20319418x10^{7}	$B_{5,co}$=1.34966306x10^{9}
a_6=1.838826904x10^{-10}		

table 2. Coefficients for the alternative equations of state.

constituent	density (g·cm^{-3})
H_2O Ic (cubic)	0.96
H_2O Ih (hexagonal)	0.92
a-H20(amorphous)	1.1*
}12011	1.17**
CO	2.106
CO_2	1.69

table 1. Densities of ice phases used with the model. The amorphous ice reference is from *Klinger [1982], and the ice II reference is from ** Poirier et al. [1982], The others are from standard references except for that of CO which was derived.

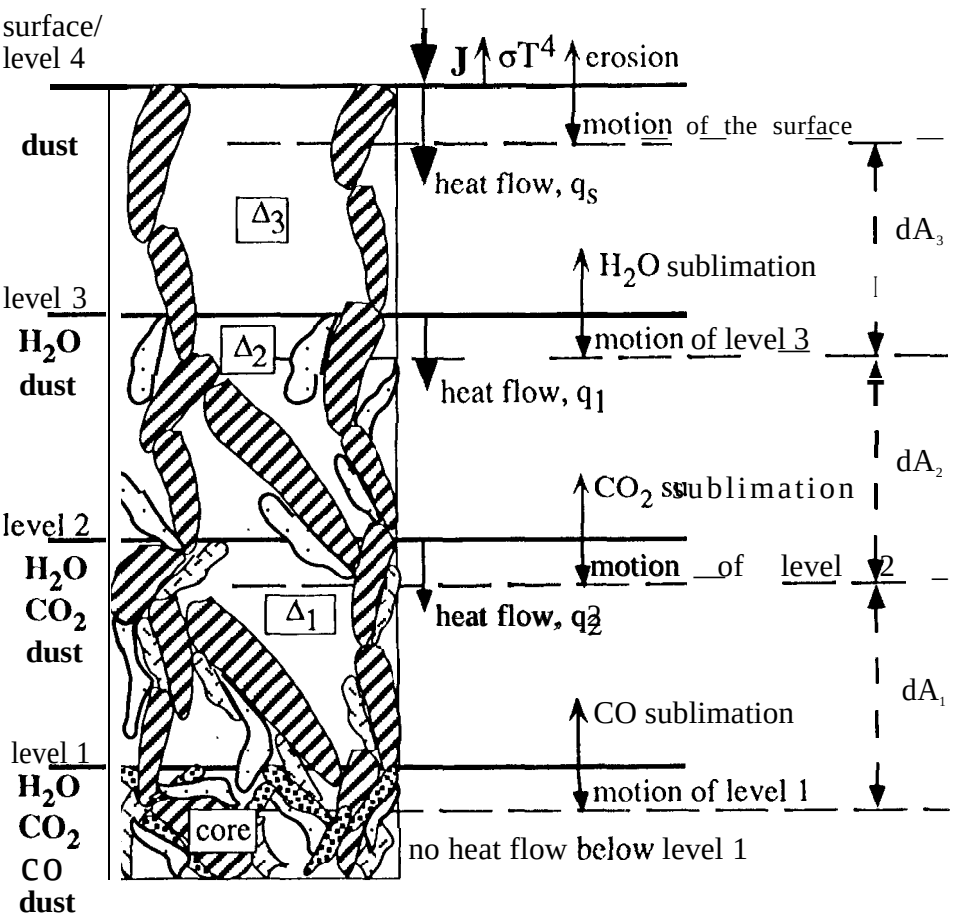

figure 1. A schematic showing a possible comet nucleus structure and the evolution of the sublimation process as proposed by the model with separated comet mantles. Silicate grains are shown, overlain by frozen ices from which gaseous molecules of various species may sublime. The large, heavily striped grains depict silicate dust particles. Water ice is shown with dotted markings, C02 ice by short dashes, and CO ice by heavy dots, Three layers are illustrated. As heat impinges on the surface, the most volatile gases sublimate first, etc., leaving behind a layer evacuated of that particular species. In layer 1 the unevaluated species are C02 and H20, in layer 2 the unevaluated is H20. Layer 3 is completely evacuated of volatiles. The interfaces between layers are parallel to the surface. Mass change due to sublimation at the different levels results in motion of the level surface. The dashed lines indicate the new location of the sublimating surface after sublimation has occurred. The change in location of the sublimating surface is denoted dA. As gas production proceeds, leaving behind increasingly thickened mantles if the production is rapid, the increased insulation may have the effect of choking off the production itself such that the layer thins again. Thus the growth and shrinkage of the mantles is modeled as a time dependent effect.

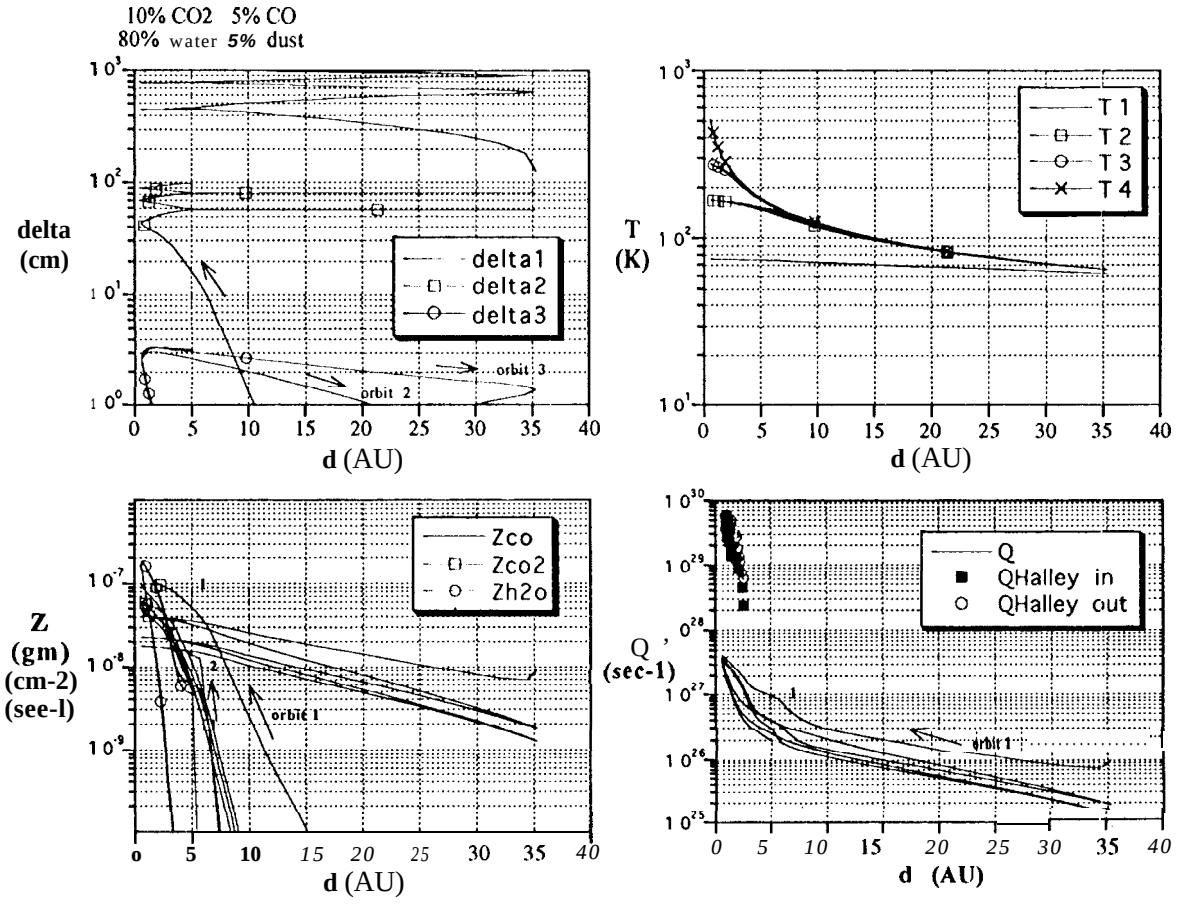

figure 2. A case with 80% water, 5% CO, and 10% C02 is shown. The dust content is 5% and the porosity is O%. The innermost mantle maintains a thickness of several 10's of meters throughout the orbit. The total gas production is taken to the the sum of the gas production rates multiplied by the size of a typical active area of 50 km^2. Halley data are reproduced from Roettger et al., [1990]. The figure shows the middle mantle thickness growing to several 10's of centimeters and the top mantle growing to a thickness on the order of 3 centimeters. The temperatures separate into 4 distinct layers around 5 AU.

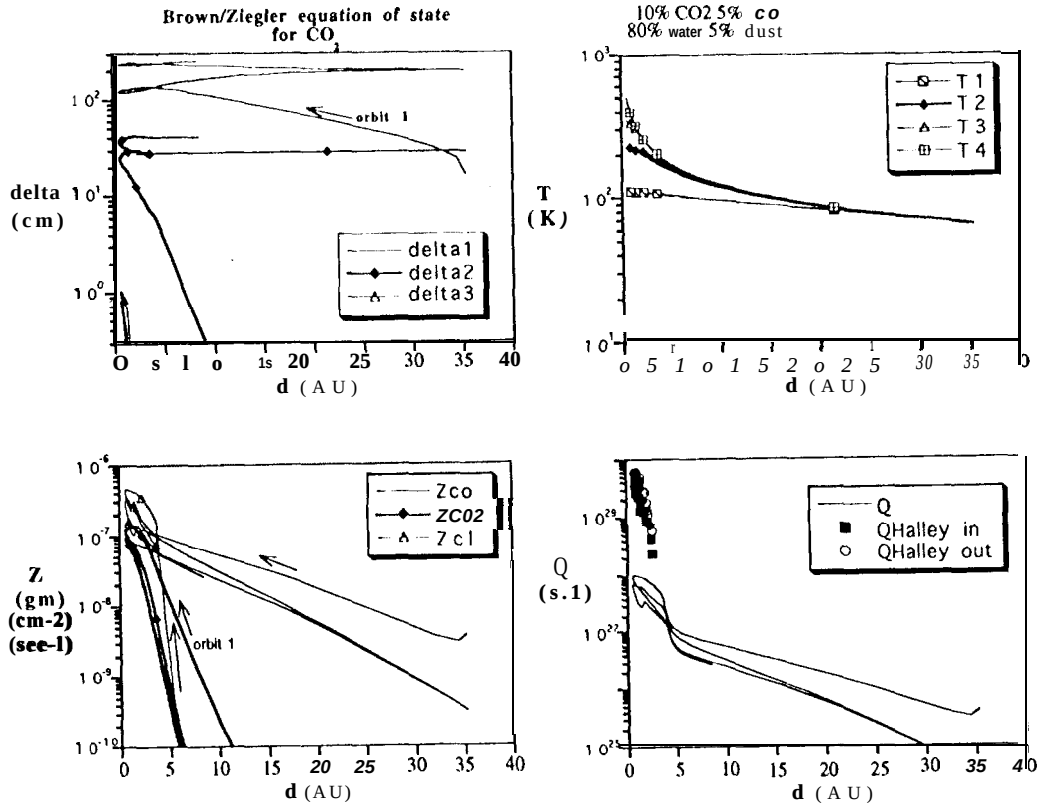

figure 3. A case with 80% water, 5% CO, 10% CO_2, and 5% dust is shown. In this case the Brown/Ziegler equation of state for C02 is assumed. C02 production is enhanced for most of the orbit, however the overall gas production solution is relatively low. The innermost mantle maintains a thickness of several 100's of meters. The middle mantle thickness grows to several 10's of centimeters and the top mantle grows to a thickness on the order of a centimeter. The temperatures separate into 4 distinct layers around 3 AU.

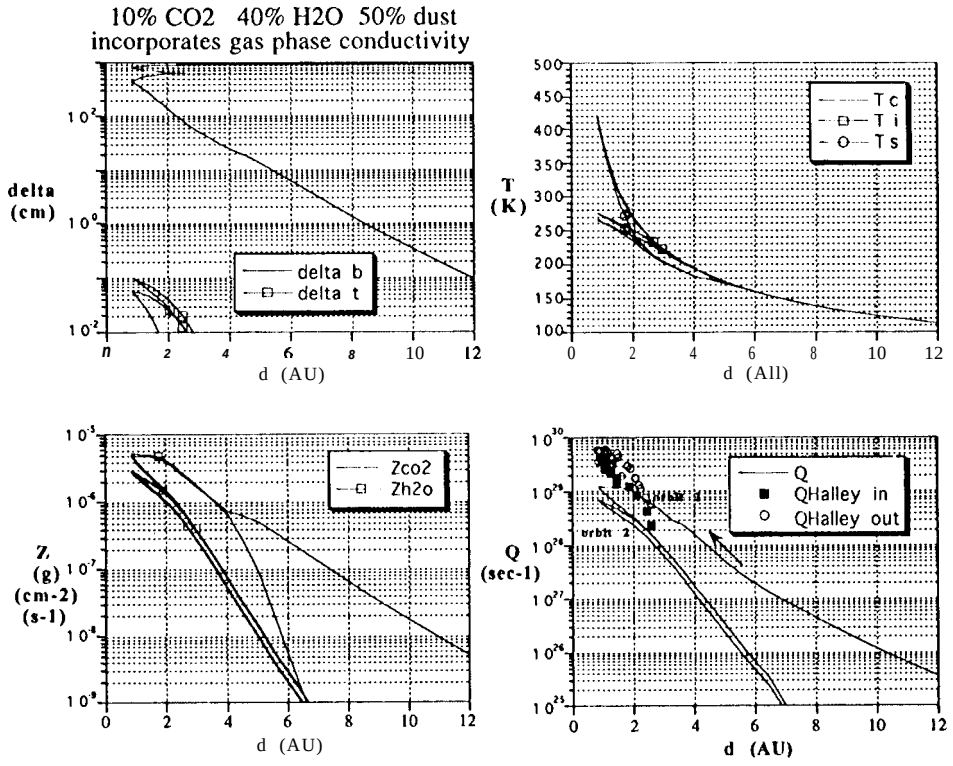

figure 4. Showing the effect of using a gas phase conductivity expression with the model. A case with 40% water, 10% C02 , and 50% dust is shown. The innermost mantle maintains a thickness of several 100s of meters throughout the orbit. The top mantle growing to a thickness on the order tenths of a centimeters. The temperatures separate into 3 distinct layers around 3 AU. Total gas production is improved significantly over the other models $\sim 10^{29}$ (see^{-1}).

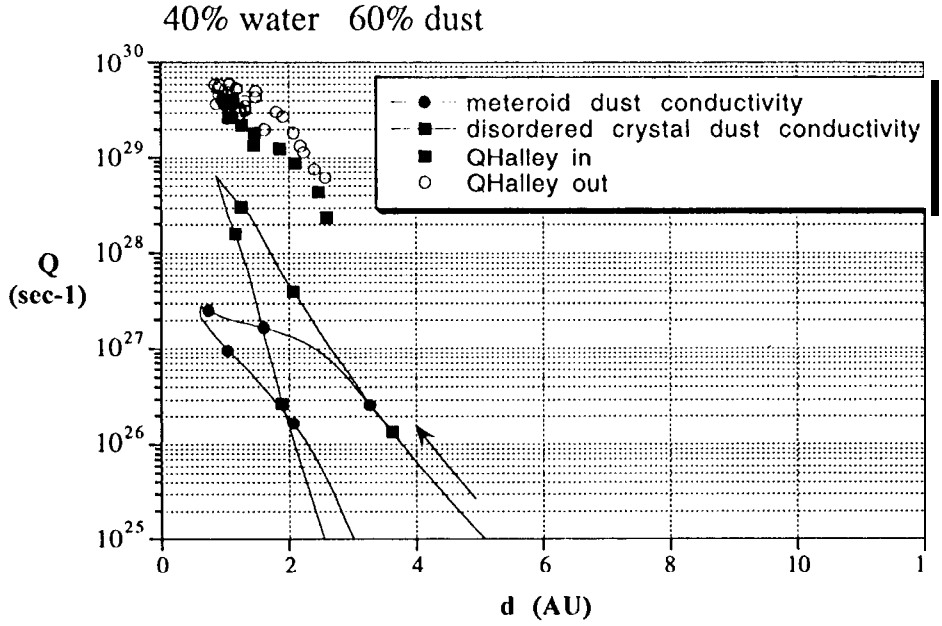

figure 5. Showing the effect of using an expression for the conductivity of the silicate grains that is based on disordered crystal structure, Cahill et al., [1980], for a water ice and dust comet. Total gas production is improved over the other water ice and dust models by an order of magnitude.

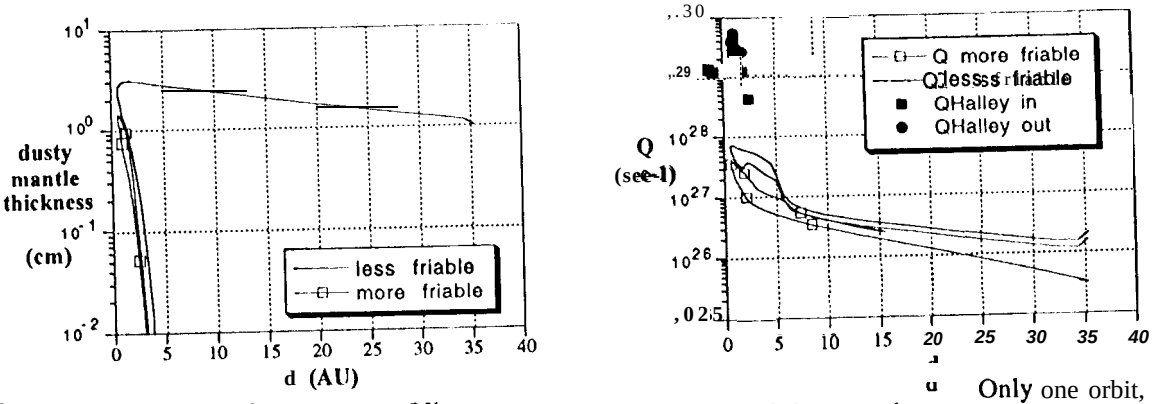

figure 6. Two cases of composition 5% C02, 10% CO, water ice, and dust are shown. Only one orbit, from -35 AU, is shown. The left panel shows the thickness of the top mantle as it changes with distance over the orbit. The more friable comet has ice exposed directly to space until very near perihelion. The comet becomes bald again shortly after perihelion. The ice sublimates freely to space and the comet is cool. The less friable comet retains a surface, dusty mantle over a larger portion of the orbit, the ice does not sublimate freely to space, interior temperatures are warmer, and near perihelion there is a greater degree of outgassing.